ChemComm

Accepted Manuscript

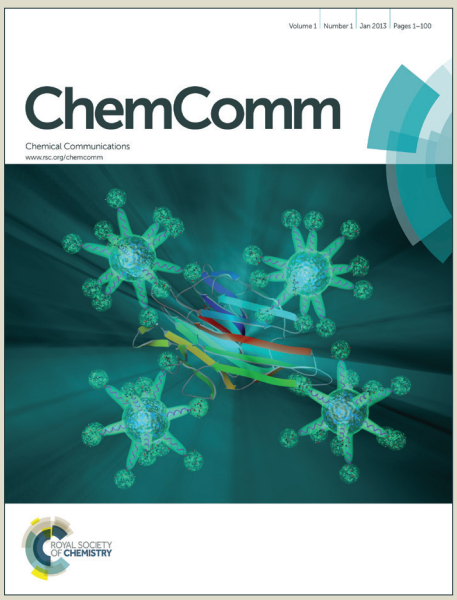

ROYAL SOCIETY OF CHEMISTRY

www.rsc.org/chemcomm

Cite this: DOI: 10.1039/c0xx00000x

www.rsc.org/xxxxxx

COMMUNICATION

Smart design of free-standing ultrathin Co/Co(OH)$_2$ composite nanoflakes on 3D nickel foam for high-performance electrochemical capacitors

Zheyin Yu,[a] Zhenxiang Cheng,*[a] Siti Rohana Majid ,[a] Zhixin Tai,[a] Xiaolin Wang,[a] and Shixue Dou [a]

Received (in XXX, XXX) Xth XXXXXXXXX 20XX, Accepted Xth XXXXXXXXX 20XX
DOI: 10.1039/b000000x

Ultrathin Co/Co(OH)$_2$ composite nanoflakes have been fabricated through electrodeposition on 3D nickel foam. As electrochemical capacitor electrode, they exhibit high specific capacitance, 1000 F/g at the scan rate of 5 mV/s and 980 F/g at the current density of 1 A/g, respectively, and the retention of capacitance is 91% after 5000 cycles.

Nowadays, tremendous research efforts have been made in energy storage and conversion from clean and renewable energy sources due to the increasing demand for such energy.[1] Electrochemical capacitors (ECs) are one type of promising energy storage device with the merits of high power density, good pulse charge−discharge characteristics, and long lifetime, which make them applicable in many portable systems and in hybrid electric vehicles.[2] There are three major types of electrode materials for ECs: carbon materials[3], metal oxides/hydroxides[4], and conducting polymers[5]. Among the various electrode materials, ruthenium oxide exhibits excellent electrochemical performance, with long lifespan and high specific capacitance.[6] Its high cost, low porosity, and toxic nature have limited its commercial application, however. Therefore, cheaper and more environmentally-friendly metal oxides/hydroxides need to be developed, such as NiO[7], Co_3O_4[8], Fe_3O_4[9], Co(OH)$_2$[10], and V_2O_5[11]. Among the inexpensive materials, Co(OH)$_2$ has been considered as a promising electrode material for ECs, owing to its well-defined redox activity, great reaction reversibility, low fabrication cost, natural abundance, and environmental friendliness. Various methods have been developed to synthesize Co(OH)$_2$, such as the hydrothermal method[12], sol-gel[13], and electrodeposition[14].

It is well known that metallic cobalt coating through electrodeposition has been widely applied in industry, but its microstructure is commonly compact and bulk-like[15], which could not satisfy the requirement for ECs with high specific surface area, although after electrodeposition of the metallic Co, the surface will be oxidized to Co(OH)$_2$[16], which is an ideal active material for ECs.

In this Communication, considering the above two characteristics, we have adopted the electrodeposition technique to fabricate ultrathin Co/Co(OH)$_2$ composite nanoflakes (CCCNs) on three-dimensional (3D) nickel foam current collector to enhance their specific surface area. The experimental process is detailed in the Electronic Supplementary Information (ESI)†. To the best of our knowledge, there have been no reports on the fabrication of such ultrathin Co/Co(OH)$_2$ composite nanoflakes and their application as electrode materials in ECs. The unique design of CCCNs for ECs electrode material possesses obvious advantages, as described below. Fig. 1 presents a schematic diagram of the structure of the CCCNs. This structure has the following advantages: (a) The un-oxidized metallic Co in each nanoflake has high electrical conductivity and provides fast paths for electron transport to the current collector, which could overcome the key shortcoming of the poor conductivity of Co(OH)$_2$. (b) The Co(OH)$_2$ and metallic Co are integrated in every flake, unlike in reports where the Co(OH)$_2$ was electrodeposited on a conductive scaffold, which means that the active materials feature excellent mechanical properties and will not fall off easily, which could keep the capacitance relatively stable during charge-discharge cycling. (c) The CCCNs directly grown on conductive nickel foam are binder-free electrode, ensuring excellent electrical contact with the current collector, which enables every Co/Co(OH)$_2$ composite nanoflake to effectively participate in electrochemical reactions and avoid the "dead" volume effect. (d) The nanoscale open pores between the Co/Co(OH)$_2$ composite flakes could enhance the transport of ions, and the ultrathin CCCNs could shorten the ion diffusion paths, thereby leading to fast, reversible Faradaic reactions. (e) The ultrathin Co/Co(OH)$_2$ composite nanoflakes could enhance the utilization rate of the active material Co(OH)$_2$, because only the metallic Co surface can be oxidized to Co(OH)$_2$. (f) The initial electrodeposited metallic cobalt on the current collector has better mechanical adhesion compared with Co(OH)$_2$, which could avoid the electrical isolation phenomenon, because the CCCNs would not detach easily from the current collector during charge-discharge cycling.

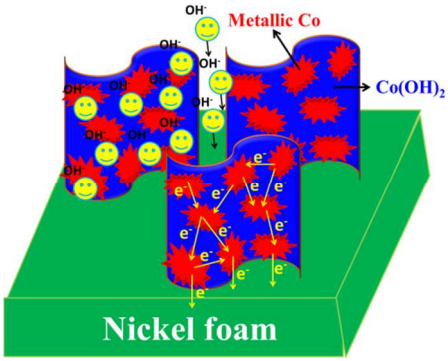

Fig. 1 Schematic diagram of ultrathin Co/Co(OH)$_2$ composite nanoflakes for ECs.

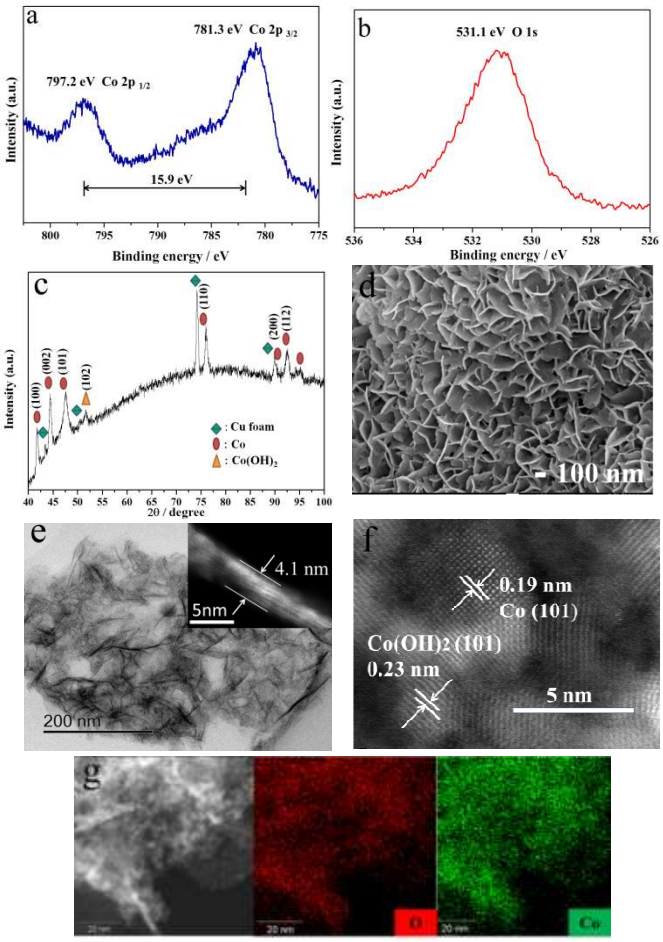

Fig. 2 XPS spectra of (a) Co 2p and (b) O 1s for the CCCNs. (c) XRD pattern of CCCNs. (d) SEM image of CCCNs. (e) STEM image of a single nanoflake, with the inset showing the thickness of a single nanoflake. (f) High resolution STEM image corresponding to (e). (g) STEM EDX mapping of O and Co.

X-ray photoelectron spectroscopy (XPS) was employed to examine the surface chemical states of CCCNs. Fig. 2(a, b) presents the Co 2p and O 1s spectra of the CCCNs, respectively. In Fig. 2(a), there are two main Co 2p peaks, which are located at binding energies of 797.2 eV (Co $2p_{1/2}$) and 781.3 eV (Co $2p_{3/2}$), and the distance between these two peaks is 15.9 eV, which indicates that the Co^{2+} exists in the form of $Co(OH)_2$. In addition, there is no apparent peak around 778 eV, suggesting that the surface species was not the metallic cobalt. Fig. 2(b) shows the binding energy of the O 1s state at 531.1 eV, which confirms the presence of O-H bonds from the $Co(OH)_2$. The XPS measurements confirm that the surface of the CCCNs is mostly covered by $Co(OH)_2$[17].

X-ray diffraction (XRD) analysis was used to determine the chemical composition and the crystalline structure of the CCCNs. Because some peaks of cobalt overlap the peaks from nickel foam, we used copper foam as the substrate for testing. In Fig. 2(c), the peaks located at 41.76°, 44.40°, 47.60°, 76.02°, 90.30°, 92.62°, and 94.72° were identical to the diffractions from hexagonal close-packed (hcp) Co (100), (002), (101), (110), (200), (112), and (201) crystal planes, respectively (JCPDS No.05-0727). The peak located at 51.68° was assigned to the $Co(OH)_2$ (102) crystal planes.

The scanning electron microscope (SEM) images in Fig. 2(d) and Fig. S2 (ESI†) show the surface morphology of the CCCNs. On the nickel foam, there are obvious vertically grown nanoflakes. Among the nanoflakes, there are uniformly distributed nanoscale open pores, approximately 60 to 200 nm in diameter, which are able to facilitate the penetration of electrolyte, reduce contact resistance, and enhance mass/charge transfer at the interface between the electrode and electrolyte. Fig. 2(e) shows a scanning transmission electron microscope (STEM) image of a single $Co(OH)_2$/Co composite nanoflake, and the inset shows that the thickness of a typical flake is about 4.1 nm, which features the advantages of shortening the diffusion distance and increasing the utilization of active materials. As can be seen from Fig. 2(f), the spacing between adjacent fringes was measured to be 0.19 nm and 0.23 nm, corresponding to hcp Co (101) crystal planes and $Co(OH)_2$ (101) crystal planes, respectively. Fig. 2(g) shows STEM energy dispersive X-ray spectroscopy (EDX) mapping analysis of O (in red colour) and Co (in green colour), which clearly indicates that the elements O and Co were uniformly distributed.

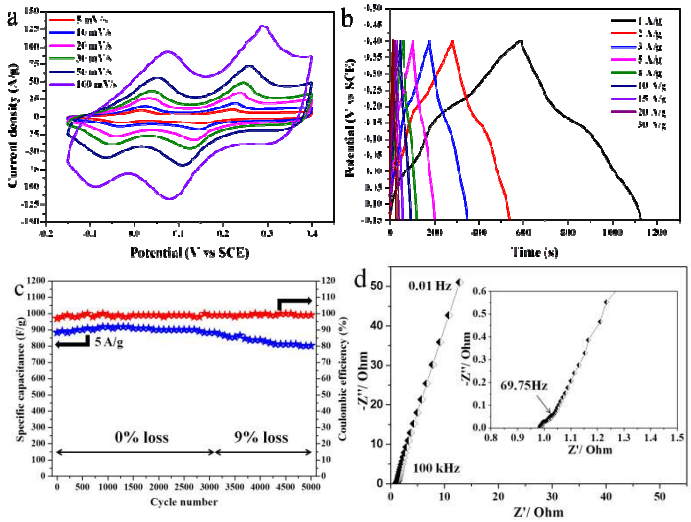

Fig. 3 Electrochemical characterization of CCCNs: (a) CV curves at various scan rates. (b) Charge-discharge curves at various current densities. (c) Cycling performance of CCCNs at the current density of 5 A/g for 5000 cycles. (d) EIS spectrum of CCCNs, with the inset showing an enlargement of the high frequency region.

Fig. 3(a) shows representative cyclic voltammetry (CV) curves of CCCNs at scan rates ranging from 5 to 100 mV/s. Well-defined redox peaks within the range of -0.15–0.4 V appear in all the curves, which demonstrates that the electrochemical capacitance is derived from pseudocapacitive Faradaic redox reactions. Two quasi-reversible electron-transfer processes are observed, which are ascribed to plausible reactions at the electrode/electrolyte interface. The first pair of peaks at about 0–0.1 V is assigned to the conversion between $Co(OH)_2$ and CoOOH: $Co(OH)_2 + OH^- \leftrightarrow CoOOH + H_2O + e^-$. The second pair of peaks at about 0.1–0.4 V is due to the conversion between CoOOH and CoO_2: $CoOOH + OH^- \leftrightarrow CoO_2 + H_2O + e^-$.[18] In Fig. S3 (ESI†), the two redox reaction peak currents (cathodic and anodic) each display linear relationships with the square root of the scan rate, indicating that the reaction is diffusion controlled and that the CCCNs have good conductivity.[19] In addition, the shape of the CV curves is not significantly influenced by increasing scan rate, even at 100 mV/s. This suggests that the CCCNs are suitable for fast redox reactions with good rate capability.[20] The specific capacitances calculated from the CV

curves (Fig S4, ESI†) are 1000 F/g, 910 F/g, 841 F/g, 801 F/g, 754 F/g, and 684 F/g for scan rates of 5, 10, 20, 30, 50, and 100 mV/s, respectively. The above data shows that approximately 68.40 % of the capacitance was still retained when the scan rate increased from 5 to 100 mV/s.

Galvanostatic charge-discharge measurements were conducted within the potential window of -0.15 to 0.4 V at a set of current densities ranging from 1 to 30 A/g. As shown in Fig. 3(b), a highly symmetric shape during the charge-discharge process was observed, and there was no apparent instantaneous potential drop at low current density, which means that the CCCNs possess excellent conductivity.[21] Moreover, there were two redox reaction regions (Co^{4+}/Co^{3+}, Co^{3+}/Co^{2+}) in all the charge-discharge curves, which is in agreement with the CV curves, indicating the good electrochemical performance. As shown in Fig. S5 (ESI†), the specific capacitance can be calculated as 980 F/g (at 1 A/g), 924 F/g (at 2 A/g), 913 F/g (at 3 A/g), 884 F/g (at 5 A/g), 852 F/g (at 8 A/g), 831 F/g (at 10 A/g), 766 F/g (at 15 A/g), 738 F/g (at 20 A/g), and 693 F/g (at 30 A/g), respectively. The above results show that approximately 70.71% of the capacitance is still retained when the charge-discharge rate is increased from 1 to 30 A/g, demonstrating the good ion diffusion and electron transport capability at high current density.[20]

Galvanostatic charge-discharge measurements were carried out for 5000 cycles at the high current density of 5 A/g between -0.15 and 0.4 V. In Fig. 3(c), it is clear that the specific capacitance is almost constant over the first 3100 cycles, and there is no capacitance loss. In the subsequent 1900 cycles, the capacitance only decreases by 9%. The retention of capacitance was 91 % after 5000 cycles. In addition, at the high current density of 5 A/g, the coulombic efficiency was relatively stable and high.

Fig. 3(d) shows electrochemical impedance spectra (EIS) in the form of Nyquist plots for as-prepared CCCNs electrode. It is well accepted that the equivalent series resistance (ESR) is contributed by the electrolyte resistance, the resistance of the active materials, and the contact resistance between the active materials and the current collector[3], and in this work, the ESR is 0.98 Ω, indicating the high conductivity of the CCCNs, which is due to the excellent electrical contact with the nickel foam[19]. The semicircle in the high frequency region reflects the properties of the electrode surface and indicates a charge transfer resistance (R_{ct}) of 0.08 Ω, which is relatively low. Therefore, it could be supposed that the metallic cobalt in the CCCNs provides an ideal electron pathway for fast electron transport and ensures excellent rate capability. The knee frequency [inset to Fig. 3(d)] is found to be 69.75 Hz, which indicates good reaction kinetics, since the commonly reported knee frequency is less than 10 Hz for ECs.[22]

Energy density and power density are two key factors in evaluating the suitability of a material for ECs application. A good electrode material is expected to provide high power density and high capacitance simultaneously at high charge-discharge rates. Therefore, a Ragone plot (showing the relationship between the energy density and the power density) is presented in Fig. S6 (ESI†). It can be observed that, with increased power density, the energy density is slowly reduced, reaching 41.19 Wh/kg at a power density of 0.28 kW/kg, but still retaining 29.10 Wh/kg at a power density of 8.25 kW/kg, which could be attributed to the excellent rate capability.

In summary, we successfully fabricated free-standing ultrathin $Co/Co(OH)_2$ composite nanoflakes on 3D nickel foam through electrodeposition for application in ECs. The CCCNs exhibited excellent electrochemical performance. The capacitance was calculated to be 1000 F/g at the scan rate of 5 mV/s and 980 F/g at the galvanostatic charge-discharge current density of 1 A/g, while the rate capability was 68.40% at the scan rate of 100 mV/s and 70.71% at the galvanostatic charge-discharge current density of 30 A/g, respectively. In addition, the excellent mechanical adhesion between the CCCNs and the nickel foam, and the $Co/Co(OH)_2$ composite nanoflake structure ensure that the capacitance remains stable during 5000 charge-discharge cycles. We designed the $Co/Co(OH)_2$ composite nanoflakes on nickel foam to achieve high specific capacitance, good rate capability, and excellent cycling performance at the same time, and the cycling performance is particularly outstanding compared with reported works (Table S7, ESI†), providing a new way to fabricate electrode materials for ECs with high performance.

The authors are grateful to Dr. Tania Silver for carefully polishing the paper，and Tony Romeo and Gilberto Casillas-Garcia for the help in SEM and STEM testing. ZX Cheng thanks the Australian Research Council (ARC) for support.

Notes and references

[a] *Institute for Superconducting and Electronic Materials, University of Wollongong, Wollongong, Australia. Fax: 61 2 4221 5731; Tel: 61 2 4298 1406; E-mail: cheng@uow.edu.au*

† Electronic Supplementary Information (ESI) available: [details of any supplementary information available should be included here]. See DOI: 10.1039/b000000x/

1 (a) J. Jiang, J. Zhu, W. Ai, Z. Fan, X. Shen, C. Zou, J. Liu, H. Zhang and T. Yu, *Energy & Environmental Science*, 2014, **7**, 2670; (b) J. Liu, J. Jiang, C. Cheng, H. Li, J. Zhang, H. Gong and H. J. Fan, *Adv Mater*, 2011, **23**, 2076; (c) S. Luo, K. Wang, J. Wang, K. Jiang, Q. Li and S. Fan, *Adv Mater*, 2012, **24**, 2294; (d) C. Zhou, Y. Zhang, Y. Li and J. Liu, *Nano Lett*, 2013, **13**, 2078.

2 (a) J. Liu, G. Cao, Z. Yang, D. Wang, D. Dubois, X. Zhou, G. L. Graff, L. R. Pederson and J. G. Zhang, *ChemSusChem*, 2008, **1**, 676; (b) J. R. Miller and P. Simon, *Science*, 2008, **321**, 651.

3 L. L. Zhang and X. S. Zhao, *Chem Soc Rev*, 2009, **38**, 2520.

4 H. Jiang, T. Zhao, C. Li and J. Ma, *J Mater Chem*, 2011, **21**, 3818.

5 I. Kovalenko, D. G. Bucknall and G. Yushin, *Advanced Functional Materials*, 2010, **20**, 3979.

6 C.-C. Hu, K.-H. Chang, M.-C. Lin and Y.-T. Wu, *Nano Lett*, 2006, **6**, 2690.

7 B. Qu, L. Hu, Y. Chen, C. Li, Q. Li, Y. Wang, W. Wei, L. Chen and T. Wang, *Journal of Materials Chemistry A*, 2013, **1**, 7023.

8 X.-h. Xia, J.-p. Tu, Y.-j. Mai, X.-l. Wang, C.-d. Gu and X.-b. Zhao, *Journal of Materials Chemistry*, 2011, **21**, 9319.

9 D. Liu, X. Wang, X. Wang, W. Tian, J. Liu, C. Zhi, D. He, Y. Bando and D. Golberg, *Journal of Materials Chemistry A*, 2013, **1**, 1952.

10 C. Mondal, M. Ganguly, P. K. Manna, S. M. Yusuf and T. Pal, *Langmuir*, 2013, **29**, 9179.

11 B. Saravanakumar, K. K. Purushothaman and G. Muralidharan, *ACS Appl Mater Interfaces*, 2012, **4**, 4484.

12 Y. Yao, C. Xu, S. Miao, H. Sun and S. Wang, *J Colloid Interface Sci*, 2013, **402**, 230.

13 N. Özer, D.-G. Chen and T. Büyüklimanli, *Solar Energy Materials and Solar Cells*, 1998, **52**, 223.

14 T. Zhao, H. Jiang and J. Ma, *Journal of Power Sources*, 2011, **196**, 860.

15 (a) Q. Chu, W. Wang, J. Liang, J. Hao and Z. Zhen, *Materials Chemistry and Physics*, 2013, **142**, 539; (b) N. R. Nik Masdek and A. M. Alfantazi, *Journal of Solid State Electrochemistry*, 2014, **18**, 1701; (c) R. Pinto, M. J. Carmezim and M. F. Montemor, *Journal of Power Sources*, 2014, **255**, 251; (d) L. Wang, Y. Gao, H. Liu, Q. Xue and T. Xu, *Surface and Coatings Technology*, 2005, **191**, 1.

16 (a) A. Amri, Z.-T. Jiang, P. A. Bahri, C.-Y. Yin, X. Zhao, Z. Xie, X. Duan, H. Widjaja, M. M. Rahman and T. Pryor, *The Journal of Physical Chemistry C*, 2013, **117**, 16457; (b) P. Bera, H. Seenivasan, K. S. Rajam and V. K. William Grips, *Applied Surface Science*, 2012, **258**, 9544; (c) K. Sharifi and M. Ghorbani, *Bull*

Mater Sci, 2014, **37**, 713.
17 (a) H.-J. Ahn, W. B. Kim and T.-Y. Seong, *Electrochemistry Communications*, 2008, **10**, 1284; (b) T. Xue, X. Wang and J.-M. Lee, *Journal of Power Sources*, 2012, **201**, 382.
18 V. Srinivasan and J. W. Weidner, *Journal of Power Sources*, 2002, **108**, 15.
19 G. Zhang, W. Li, K. Xie, F. Yu and H. Huang, *Advanced Functional Materials*, 2013, **23**, 3675.
20 (a) J. H. Kim, K. Zhu, Y. Yan, C. L. Perkins and A. J. Frank, *Nano Lett*, 2010, **10**, 4099; (b) X. Tian, C. Cheng, L. Qian, B. Zheng, H. Yuan, S. Xie, D. Xiao and M. M. F. Choi, *Journal of Materials Chemistry*, 2012, **22**, 8029.
21 A. K. Singh, D. Sarkar, G. G. Khan and K. Mandal, *Journal of Materials Chemistry A*, 2013, **1**, 12759.
22 (a) B. Tao, J. Zhang, F. Miao, S. Hui and L. Wan, *Electrochimica Acta*, 2010, **55**, 5258; (b) F. Tao, Y.-Q. Zhao, G.-Q. Zhang and H.-L. Li, *Electrochemistry Communications*, 2007, **9**, 1282; (c) Y.-g. Wang and Y.-y. Xia, *Electrochimica Acta*, 2006, **51**, 3223; (d) T.-Y. Wei, C.-H. Chen, K.-H. Chang, S.-Y. Lu and C.-C. Hu, *Chemistry of Materials*, 2009, **21**, 3228.